Observation of zigzag and armchair edges of graphite using scanning tunneling microscopy and spectroscopy

Yousuke Kobayashi,[1,*] Ken-ichi Fukui,[1] Toshiaki Enoki,[1] Koichi Kusakabe,[2] and Yutaka Kaburagi[3]
[1]*Department of Chemistry, Tokyo Institute of Technology, 2-12-1, Ookayama, Meguro-ku, Tokyo 152-8551, Japan*
[2]*Graduate School of Engineering Science, Osaka University, 1-3, Machikaneyama-cho, Toyonaka, Osaka 560-8531, Japan*
[3]*Department of Energy Science and Engineering, Musashi Institute of Technology, 1-28-1, Tamazutsumi, Setagaya-ku, Tokyo 158-8557, Japan*
(Received 14 February 2005; published 25 May 2005)

The presence of structure-dependent edge states of graphite is revealed by both ambient and ultrahigh-vacuum (UHV) scanning tunneling microscopy and scanning tunneling spectroscopy observations. On a hydrogenated zigzag (armchair) edge, bright spots are (are not) observed together with a $(\sqrt{3}\times\sqrt{3})R30°$ superlattice near the Fermi level ($V_S\sim-30$ mV for a peak of the local density of states) under UHV, demonstrating that a zigzag edge is responsible for the edge states, although there is no appreciable difference between as-prepared zigzag and armchair edges in air. Even in the hydrogenated armchair edge, however, bright spots are observed at defect points, at which partial zigzag edges are created in the armchair edge.

DOI: 10.1103/PhysRevB.71.193406 PACS number(s): 73.20.At, 68.65.−k

Finite-sized graphene has attracted attention for its peculiar electronic structure dependent on the dimensionality, size, and geometry. The interference effect on electronic wave functions can be dominant for two-dimensional (2D) structures, dependent on the sample size.[1,2] Periodic contrast of the density of states (DOS) of carbon nanotubes, which consist of graphene rolled with chiral vectors, is due to the electronic confinement effect appearing in the 1D electronic structure.[3] On top of those interference effects, edge-localized electronic states are more characteristic. Especially when those materials become smaller, the electronic structure drastically changes in the case of nanometer-long carbon nanotubes or nanometer-wide graphene ribbons.[4,5] An analytical model for the distribution of edge-localized electrons of graphene and their density of states were proposed by Fujita and co-workers.[5–7] According to the model, the nonbonding π electrons at a zigzag edge can be delocalized toward the interior of the plane with a finite probability density, which is dependent on the wave number of the edge states. The edge states make almost flat bands near the Fermi level in addition to the π and π^* bands of graphene. Ferromagnetism can arise by an arrangement of the spins of nonbonding π electrons at a zigzag edge of nanographene or graphene ribbons, on assumption of a model of bipartite lattices.[8,9] In contrast, those interesting characters are quite absent at an armchair edge. The peculiar local DOS (LDOS) due to the edge states near the zigzag edge is supported by some experimental reports, for example, on disordered magnetism of activated carbon fibers or shouldered I-V_S curves near the Fermi level of a hydrogen-irradiated graphite step edge. However, the origin of the atomic-structure-dependent LDOS, which is a key to solving the unconventional electronic structure and magnetism, remains unclear.[10,11] Therefore direct observation of local electronic structure near an edge is the most important issue in clarifying the characters of edge states which relate to the experimental findings. An atomically resolved study about the edges of graphite will be a strong support to previous theoretical and experimental papers and create a different appraoch to nanomaterials of graphite and its related materials. In the present Brief Report, we show scanning tunneling microscope (STM) images of zigzag and armchair edges of graphite near the Fermi level and dI/dV_S curves from scanning tunneling spectroscopy (STS) to observe the distribution of edge-localized electrons and edge states, accompanied with the theoretically calculated LDOS mapping to reproduce the experimental images.

All atomically resolved STM images in constant-height mode were taken at $V_S=0.02$ V and $I=0.7$ nA, using a Pt-Ir tip by Nanoscope E (Digital Instruments Co.) and UHV STM (Unisoku Co.) for observations in air and under UHV conditions, respectively. The sample preparation of nanographite is given elsewhere.[12] In the sample preparation process, pits can also be generated due to reaction of the residue of oxygen with the highly oriented pyrolitic graphite (HOPG) substrate surfaces during the heat treatment.[13] The samples were exposed to air after the sample preparation. As for the observation under UHV conditions ($\sim5\times10^{-11}$Torr), the prepared samples were heated at around 800 °C to eliminate functional groups including oxygen in the form of CO,[14] immediately followed by exposure to atomic hydrogen to terminate the edges of graphite in a sample treatment chamber (under UHV conditions) connected to the STM observation chamber. The conditions for the hydrogenation of the edges were the same as those for hydrogenation of the Si(100) surface to make a monohydride surface.[15] Adsorbed contaminants, which were introduced in the process of sample preparation of nanographite on the HOPG substrate or by exposure to air, on the edges and graphite surface can be removed by reaction with pure hydrogen during the hydrogenation process. By several repeats of the heat treatments and hydrogenation in the preparation chamber, the structure of the edges is arranged due to the removal of hydrocarbons from hydrogen-terminated edges.[16,17]

The dispersion relation and 2D LDOS mapping were calculated using the tight-binding approximation for *AB*-stacked

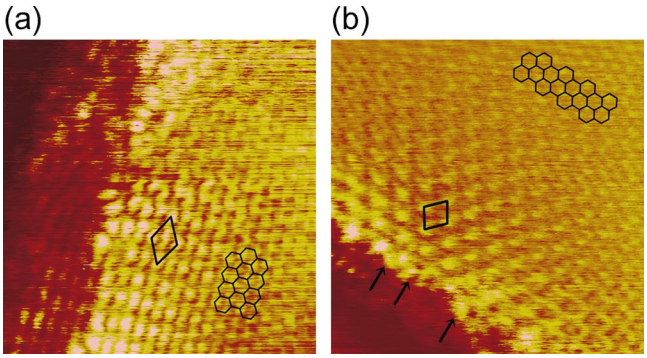

FIG. 1. (Color) Atomically resolved ambient STM images (5.6×5.6 nm^2) of (a) zigzag and (b) armchair edges of nanographene. For clarity of edge structures, models of the honeycomb lattice and $(\sqrt{3}\times\sqrt{3})R30°$ superlattice are drawn on the images and arrows are drawn to indicate irregular points at the armchair edge.

double-layer graphene. The first layer represents the top graphene layer with edges and the second layer represents the graphite substrate. The resonance integral and the overlap integral were parametrized using the Slater-Koster parameters[18] and were determined for the 2*s* and 2*p* orbitals of carbon and the 1*s* orbital of hydrogen. The structural dependence of the parameters was determined following the previous literature for carbon.[19] For carbon-hydrogen bonding, we fitted the parameters of hydrogen to reproduce the band structure of graphene strips with zigzag edges obtained by a first-principles calculation with the local density

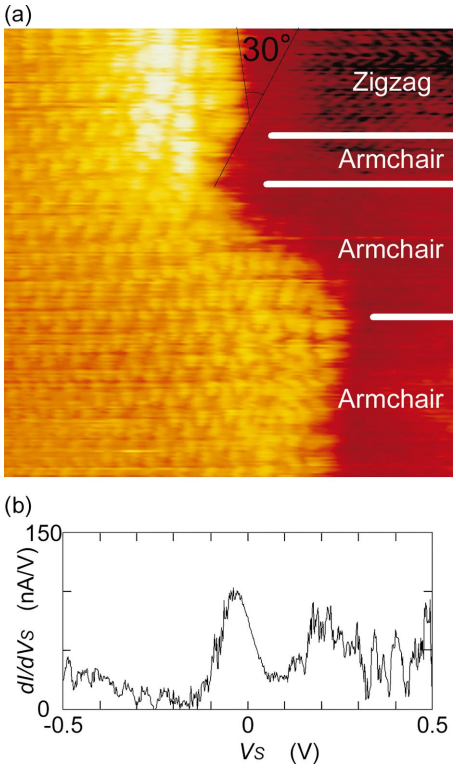

FIG. 2. (Color) (a) An atomically resolved UHV STM image of zigzag and armchair edges (9×9 nm^2). (b) Typical dI/dV_S curve from STS data at a zigzag edge.

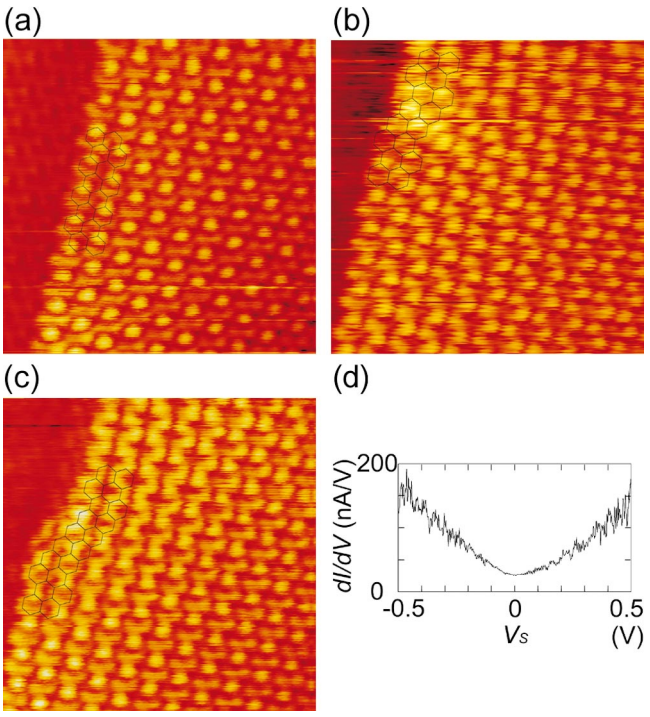

FIG. 3. (Color) Atomically resolved UHV STM images (5.6×5.6 nm^2) of (a) homogeneous armchair edge and (b), (c) armchair edges with defect points. Two and four rows of armchair lines are added to the lower regions of the edges that start from the defect points in (b) and (c), respectively. For clarity of edge structures, models of the honeycomb lattice are drawn on each image. (d) A dI/dV_S curve from STS taken at the edge in (a).

approximation.[20,21] Several percentage points of displacement of carbon atoms near each edge were neglected in the Hückel aprroximation. This makes the calculation tractable without harming essential features in the DOS.

The obtained nanographene on a highly oriented pyrolitic graphite substrate tends to have straight edges or polygonal structures. It is not difficult to find peculiar edge structures even in air. Figure 1 shows atomically resolved ambient STM images of the edges of nanographene whose diameter is about 50 nm for (a) and about 100 nm for (b). From the arrangement of the honeycomb lattice or $(\sqrt{3}\times\sqrt{3})R30°$ superlattice drawn in Fig. 1, the edges are of zigzag and armchair type for (a) and (b), respectively. Bright spots were observed near both edges, in contrast to the theoretical prediction that those bright spots can be generated only by localized electrons at a zigzag edge.[4,5] Some irregular spots were observed near bright spots of the superlattice of an armchair edge in Fig. 1(b). They are situated at positions with smaller distances than the distance of nearest-neighbor β atoms (0.246 nm). dI/dV_S curves in STS could not be obtained on both edges with reproducibility.

Figure 2(a) shows an atomically resolved UHV STM image of a hydrogenated step edge of HOPG. While no apparent contrast in spots was observed at the center and bottom parts of the edge, bright spots were observed at the top part of the edge. The top part of the edge is the zigzag type and the center and bottom parts correspond to the armchair type, judged from application of the hexagonal lattice to the image

near the edge. A typical dI/dV_S curve near the bright spots is shown in Fig. 2(b). Peaks at about −0.03 and 0.2 eV were obtained accompanied with a little contribution from the LDOS of π and π^* bands of graphite.

Figures 3(a)–3(c) show atomically resolved UHV STM images of parts of hydrogenated step edges of a pit, which is generated by reaction with residual oxygen during the sample preparation and is about 40×70 nm^2 in size. They are armchair edges of graphite, judged from the lattice information near the edges. The dI/dV_S curve at the edge of Fig. 3(a) is shown in Fig. 3(d). Only the LDOS of π and π^* bands was observed and the contribution of peaks similar to that in Fig. 2(b) was negligibly small. In contrast to the image of the homogeneous armchair edge, that of defective armchair edges in Figs. 3(b) and 3(c) is obviously different. An array of bright spots, which shows decreasing LDOS toward the interior of the plane along a line with an angle of 60° from the armchair edge, was observed at defect points in Fig. 3(b). The defect consists of an increase of two added rows of carbon atoms to the armchair edge. However, such an array was not observed near the defect points in Fig. 3(c), where four rows of carbon atoms are added.

The discrepancy between the theoretical prediction and the ambient observations in Fig. 1 is due to random oxidation of the edges and adsorption of impurity atoms or molecules at the edges by exposure to air. The chemisorbed functional groups, including oxygen atoms, change the LDOS at the edges. As another explanation for the discrepancy, one might think that the structure of the carbon network at the observed armchair edge is destroyed because edge states can be observed depending on edge structures near the Fermi level if the as-prepared edges are hydrogen terminated.[4] However, this is less suited for the description of Fig. 1(b), since we cannot specify the origin of the irregularity in the image as well as the bright spot damping toward the interior of the plane. To determine whether the edge states exist or not, we are required to specify the structure of edges under UHV conditions.

The LDOS dependence on the edge structures is clearly shown in Fig. 2(a), which is possible only for hydrogen-terminated samples under the UHV conditions. The microscopy images prove that the edge states can be observed at a homogeneous zigzag edge and at a part of the armchair edge perturbed by an adjacent zigzag edge, but they are not at armchair edges distant from other zigzag edges. The images, including the $(\sqrt{3}\times\sqrt{3})R30°$ superlattice, of homogeneous zigzag and armchair edges can be reproduced using the calculated data in Ref. 22. The image of armchair edges in Fig. 2(a) is not homogeneous because the armchair edges are perturbed by the adjacent zigzag edge and corner points. The STS data of Fig. 2(b) clearly verifies the presence of the edge states at the zigzag edge. In the figure, one peak at about −0.03 V corresponds to that of edge states and indicates the flat band near the Fermi level in the theory in Refs. 5 and 7. Taking the rapid decay of the measured current from the edge to the interior of the plane into consideration, the flat band appears to be mainly around the $k=\pi$ state, because the LDOS for the $k=2\pi/3$ state oscillates and does not decay.[5] The origin of another peak at 0.2 V in Fig. 2(b) is attributed to charge transfer from a zigzag edge to physisorbed atoms or molecules. Taking into account the facts that the hydrogenation process and the following STS observation are not completely free of impurity species and that the obtained STS data include few changes in relative position between the tip and the sample due to the thermal drift, this interpretation is reasonable.[11] Figure 3(a) clearly shows that a homogeneous hydrogenated armchair edge is created under the UHV conditions. These facts demonstrate that the edge states are not observed on the homogeneous armchair edge, but the dI/dV_S value of STS is not necessarily zero near the Fermi level due to the small charge transfer between the edge and the interior of the plane and due to weak three-dimensionality of the graphene layers.

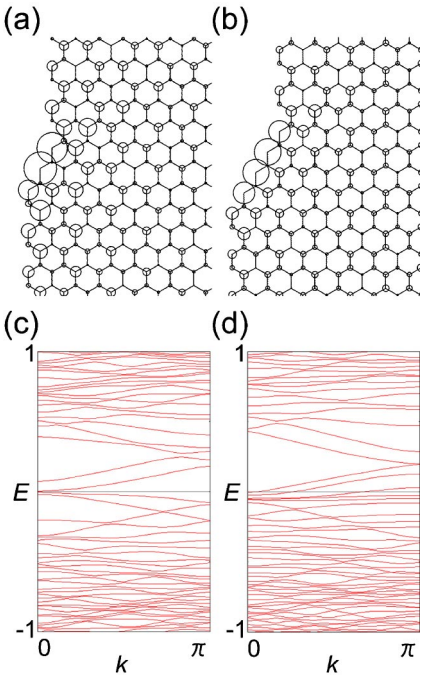

FIG. 4. (a), (b) 2D mappings of the LDOS that reproduce the observed STM images using a tight-binding approximation for *AB*-stacked double-layer graphene; (a) and (b) correspond to the images of Figs. 3(b) and 3(c), respectively. The dimension of the circle on each lattice point denotes the relative value of the LDOS that is accumulated in the range of 50 meV near the Fermi level. The energy dispersions of (a) and (b) are shown in (c) and (d), respectively.

The origins of the bright points in Figs. 3(b) and 3(c) are understood by looking at the LDOS of defect points of armchair edges. The shape of these defects is shown as increased rows of carbon atoms, as described by the honeycomb lattice drawn in Figs. 3(b) and 3(c). We show 2D mappings of the LDOS of these defect structures in Figs. 4(a) and 4(b). The tight-binding approximation for *AB*-stacked double-layer graphene is applied for the analysis, where the edges are armchair type with two and four extra rows attached to the lower half of the armchair edge in Figs. 4(a) and 4(b), respectively. From these two figures, the center of distribution of the relatively large LDOS corresponds to the defect point of the increase of two or four rows of armchair edges, that is, a partial zigzag edge embedded in an armchair edge. In Fig. 4(a), the mapping of the calculated LDOS shows a dispersed

inclination of edge electrons and it roughly reproduces Fig. 3(b), although it fails to reproduce the angle of strong directivity of the bright points in Fig. 3(b). Contrasted to the case of an increase of two rows, Fig. 4(b) shows a localized inclination of edge electrons and it well reproduces isolated bright points, which are observed in Fig. 3(c), at the point of increase of four rows. The figure also reproduces the $(\sqrt{3} \times \sqrt{3})R30°$ superlattice near the point. The distribution of the LDOS, which depends on the shape of the defect points in Figs. 3(b) and 3(c), can be attributed to that around points at $k=0$, which is shown in the crossing points in Figs. 4(c) and 4(d).

A possible explanation for the difference of the directivity is given by the different edge structure at the defect points.[23] Judged from the fabrication of the hydrogenated edge, it is possible that some extra carbon atoms remain to bind to the defect points during the heat treatment process under the UHV conditions. The carbon adatoms may change the electronic structure near the defect point. The array in Fig. 3(b) is not observed in Fig. 3(c). This may be because the edge states are energy shifted or removed due to physisorption (or chemisorption) of atomic (or molecular) species. Another possible explanation may be given by the imperfectness of the hydrogen-terminated edge. Because hydrogen, which terminates graphene edges, cannot be detected near the Fermi level by STM, it is possible that some of the edges are hydrogen deficient. In that case, dangling-bond states can be generated. The Fermi level may be shifted downward, if dangling-bond states exist. An array of bright spots similar to that in Fig. 3(b) was observed by STM around a single or a few atomic defects in graphene.[24,25] It is known that the direction of an array of bright spots around atomic defects in graphene depends on the underlying structure of carbon layers. Actually, the image of a defect point taken at an α site is different from that at a β site.[26] A similar effect is expected for a structure with a defective edge, and the directivity of the array in Fig. 3(b) may be understood as the site dependence of the defective edge.

In summary, edge states, which are dependent on edge structures, of graphene layers have been investigated by STM and STS. The edge states near the Fermi level are observed at a zigzag edge and defect points of an armchair edge. The edge states are not observed at a homogeneous armchair edge, although a $(\sqrt{3}\times\sqrt{3})R30°$ superlattice is observed dependent on the electronic states of the surroundings. Those experimental results reveal the dependence of the LDOS and the edge states of graphene layers on the edge structures. Other forms of edges of graphene can give a wide variety of LDOSs near the edges near the Fermi level. To clarify the edge states of graphene, more experimental efforts are needed, that is, investigation of another periodic form of edges, another type of edge defect, or edges terminated with another chemical species, in the near future.

The authors are grateful to Hideo Aoki for fruitful discussion. They also thank A. Moore for his generous gift of the HOPG substrate. The present work was supported by Grant-in-Aid for Scientific Research No. 15105005 from the Ministry of Education, Culture, Sports, Science, and Technology, Japan.

*Electronic address: ykobaya@chem.titech.ac.jp

[1] Y. Harigaya, Y. Kobayashi, K. Takai, J. Ravier, and T. Enoki, J. Phys.: Condens. Matter **14**, L605 (2002).
[2] Y. Kobayashi, K. Takai, K. I. Fukui, T. Enoki, K. Harigaya, Y. Kaburagi, and Y. Hishiyama, Phys. Rev. B **69**, 035418 (2004).
[3] S. Lemay, J. Janssen, M. van der Hout, M. Mooji, M. Bronikowski, P. Willis, R. Smalley, L. Kouwenhoven, and C. Dekker, Nature (London) **412**, 617 (2001).
[4] S. Okada and A. Oshiyama, J. Phys. Soc. Jpn. **72**, 1510 (2003).
[5] K. Nakada, M. Fujita, G. Dresselhaus, and M. S. Dresselhaus, Phys. Rev. B **54**, 17954 (1996).
[6] K. Kobayashi, Phys. Rev. B **48**, 1757 (1993).
[7] K. Wakabayashi, M. Fujita, H. Ajiki, and M. Sigrist, Phys. Rev. B **59**, 8271 (1999).
[8] K. Harigaya and T. Enoki, Chem. Phys. Lett. **351**, 128 (2002).
[9] K. Kusakabe and M. Maruyama, Phys. Rev. B **67**, 092406 (2003).
[10] Y. Shibayama, H. Sato, T. Enoki, and M. Endo, Phys. Rev. Lett. **84**, 1744 (2000).
[11] Z. Klusek, Z. Waqar, E. Denisov, T. Kompaniets, I. Makarenko, A. Titkov, and A. Bhatti, Appl. Surf. Sci. **161**, 508 (2000).
[12] A. Affoune, B. Prasad, H. Sato, T. Enoki, Y. Kaburagi, and Y. Hishiyama, Chem. Phys. Lett. **348**, 17 (2001).
[13] Z. Klusek, Appl. Surf. Sci. **125**, 339 (1998).
[14] K. Moriguchi, S. Munetoh, M. Abe, M. Yonemura, K. Kamei, A. Shintani, and Y. Maehara, J. Appl. Phys. **88**, 6369 (2000).
[15] J. Boland, Surf. Sci. **261**, 17 (1992).
[16] T. Zecho, A. Güttler, and J. Küppers, Carbon **42**, 609 (2004).
[17] T. Zecho, A. Güttler, X. Sha, B. Jackson, and J. Küppers, J. Chem. Phys. **117**, 8486 (2002).
[18] J. C. Slater and G. Koster, Phys. Rev. **94**, 1498 (1954).
[19] D. Papaconstantopoulos, M. Mehl, S. Erwin, and M. Pederson, in *Tight-Binding Approach to Computational Materials Science*, edited by P. E. A. Turchi, A. Gonis, and L. Colombo, MRS Symposia Proceedings No. 491 (Materials Research Society, Pittsburgh, 1998), p. 221.
[20] J. Perdew and Y. Wang, Phys. Rev. B **45**, 13 244 (1992).
[21] J. Yamauchi, M. Tsukada, S. Watanabe, and O. Sugino, Phys. Rev. B **54**, 5586 (1996).
[22] P. Giunta and S. Kelly, J. Chem. Phys. **114**, 1807 (2001).
[23] Y. Kobayashi, T. Fukui, T. Enoki, and K. Kusakabe (unpublished).
[24] J. Mizes and J. Foster, Science **244**, 559 (1989).
[25] P. Ruffieux, O. Gröning, P. Schwaller, L. Schlapbach, and P. Gröning, Phys. Rev. Lett. **84**, 4910 (2000).
[26] K. Kelly and N. Halas, Surf. Sci. Lett. **416**, L1085 (1998).